ACOUSTIC STREAMING AROUND A RESONANTLY-EXCITED CELL AND MIGRATION OF PARTICLES TO THE CROSS-SECTIONAL CENTER OF THE CHANNEL

A Thesis

by

KWANHYUNG LEE

Submitted to the Office of Graduate and Professional Studies of
Texas A&M University
in partial fulfillment of the requirements for the degree of

MASTER OF SCIENCE

Chair of Committee,	Raffaella Righetti
Committee Members,	Arum Han
	Michael Moreno
	Jun Zou
Head of Department,	Miroslav M. Begovic

May 2018

Major Subject: Electrical Engineering

ABSTRACT

Recently, a theoretical method was proposed to efficiently and accurately predict acoustic streaming around a resonantly-excited human cancer cell. The model also predicted that microparticles around the cell could be circulating along the acoustic streaming lines. The availability of this theoretical model allows determination of the resonance frequencies of the cell. In addition, the identified resonance frequencies are expected to be correlated with the mechanical properties of the cell such as density and compressibility.

The main focus of this work is the experimental corroboration of the previously proposed theoretical model. Validation of the theoretical model was performed by measuring and analyzing the acoustic streaming around MCF-7 breast cancer cells. For these experiments, a microfluidic device was fabricated using a photolithography technique, and cancer cells cultured with a sub-culturing process were used. The cancer cells and 2 μm Carboxylate microparticles suspended in the cell culture medium were injected into the microfluidic device. The device was then excited by a piezoelectric actuator with a sine wave in the frequency range of 20 kHz to 130 kHz. A resonance frequency range of 28.7 kHz to 42.0 kHz was measured experimentally when the microparticles were in circulatory motion around a cancer cell. The predicted resonance frequency range from simulations of the theoretical model was 28.665 kHz to 38.98 kHz, which is in good agreement with the experimental results. The slight underestimation of the theory with respect to the experiments may be due to small deviations of the cell

modeling parameters. In this work, observations related to the migration of particles to the cross-sectional center of rectangular microfluidic channel are reported. The migration is necessary in order to make all particles to flow in same velocity. For this experiment, two different acoustic wave frequencies were investigated to generate both vertical nodal line and levitation forces to microparticles/cells in the channel. This would allow the experiment setting to be more similar to the simulation setting, leading to more accurate experiment result.

ACKNOWLEDGEMENTS

I wish to express my gratitude to Prof. Yong-Joe Kim for his sincere and excellent guidance on my research and study at the Acoustic and Signal Processing Laboratory of Texas A&M University. I would like to thank to my committee chair, Prof. Raffaella Righetti for her guidance during my master degree and also want to thank to committee members, Prof. Arum Han who has helped most parts of the experiment, Prof. Michael Moreno, and Prof. Jun Zou for their helpful suggestions and comments on my thesis work.

Thanks also to my friends and colleagues for giving me valuable time and experience at Texas A&M University.

CONTRIBUTORS AND FUNDING SOURCES

This work was supported by Professor Raffaella Righetti, Professor Arum Han, and Professor Jun Zou from the Department of Electrical Engineering and Professor Yong-Joe Kim and Professor Michael Moreno of the Department of Mechanical Engineering.

The device fabricated for the experiment in section 2.1.1 was made with help from Professor Arum Han. The MCF-7 cancer cell for the experiment in section 2.1.2 was cultured with help from Professor Dong-In Kim.

There are no outside funding contributions to acknowledge related to the research and compilation of this document.

TABLE OF CONTENTS

LIST OF FIGURES

LIST OF TABLES

Page

1. INTRODUCTION

In a paper entitled "Acoustic streaming around a spherical microparticle/cell under ultrasonic wave excitation" by Liu and Kim [1], it is theoretically predicted that high-amplitude acoustic streaming can form around a cancer cell when the cancer cell is excited at its resonance frequency. In the work reported in this thesis, the high-amplitude acoustic streaming around the resonantly-excited cancer cell is experimentally validated, implicating that this phenomenon can be applied as a fast, inexpensive, and practical method to identify the cancer cell's resonance frequency.

Identifying resonance frequency of cancer cells is important and helpful because the resonance frequency information can be used to identify the cancer cell's mechanical properties such as density and compressibility. These mechanical properties also can be used to detect the metastatic potential of the cancer cells as it is found that some cancer cells with high metastatic potential have high compressibility.

Research to identify the resonance frequencies of cells or particles has been conducted for several decades. Ackerman measured the resonance frequency of Amphiuma erythrocytes by exciting them at a wide range of acoustic excitation frequencies and counting the number of dead cells [2]. The resonance frequency of the erythrocytes could then be estimated at the excitation frequency where the largest number of the dead cells was identified. This experimental method requires labor-intensive, time-consuming experimental work, e.g., counting the many dead cells at the wide excitation frequency range. Marston and Apfel measured the resonance

frequencies of p-xylene droplets by using an optical technique referred to as the rainbow interferometry [3]. However, this method can be used to measure only the first-order acoustic pressure and requires a large number of the samples that can lead to high experimental costs and low throughput.

Research for applying acoustic streaming to for microfluidic system has been also conducted for several years. Chung and Cho utilized the acoustic streaming to attach micro objects to oscillating air bubble which its movement can be easily controlled by acoustic waves in a microfluidic device [4]. Ahmed and Ozcelik applied the acoustic streaming to trap micro objects in desired places in microfluidic device [5]. Wiklund and Green could make a micro pump and micro mixer using the acoustic streaming generated around micro air bubbles [6]. Dai and Jiao used the acoustic streaming for micro machine's manipulation such as collection of HEK 293 cells to air bubbles or transport of the micro objects [7]. However, the acoustic streaming research in a microfluidic device has been conducted mostly for a streaming generated around only air bubbles.

In this thesis, it is proposed that the resonance frequencies of MCF-7 human breast cancer cells can be measured inexpensively by observing the circulatory motion of microparticles around the acoustically-excited cancer cells. In this experimental method (Fig. 1), the MCF-7 human breast cancer cells are cultured and are injected into a PDMS-silicon microfluidic chip along with the microparticles and cell culture medium. A piezoelectric (PZT) actuator attached at the bottom of the chip is then used to generate acoustic shear waves in a wide range of frequencies to excite the

cells suspended in the cell culture medium inside a microfluidic device. Then, the circulatory motion of the small microparticles around the cells will be observed using a standard microscope. This microparticle's rotational motion is induced by the acoustic streaming generated by the acoustically-excited cancer cell vibration. Although the rotational motion around cells/microparticles can be formed at any frequencies, its amplitude is not high enough to be observed by using the microscope other than at or near the resonance frequency of the cancer cell, while it can be easily observed at the resonance frequency due to high inertial force applied to the cells/microparticles. That is, the velocity amplitude of the acoustic streaming around the cancer cells can be maximized at the resonance frequency so that the acoustic streaming can exert high inertia force to the microparticles to lead to the observable rotational motion around the cell. Thus, the generation of the high-level acoustic streaming around the resonantly-excited cancer cell can be used to identify the resonance frequency of the cell through the observation of the microparticle's motion.

In the proposed method, the inexpensive microscope equipped with a video camera at 20 – 30 frames/second could be used to observe the rotational motion of the microparticles since the microparticles motion is much slower than the excitation frequency. Along with the inexpensive microfluidic device, this experimental method could thus be implemented more inexpensively than existing cell resonance measurement methods. This method also does not require any mechanical contact, with the cell, that can shift the resonance frequency of the cell, resulting in an inaccurate resonance frequency estimation.

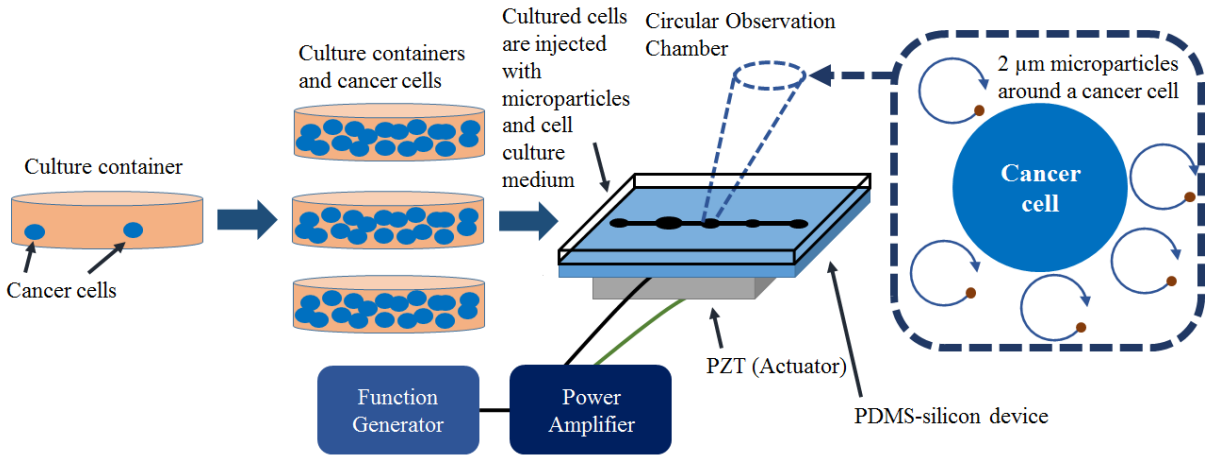

Figure 1. Overall procedure to identify resonance frequencies of MCF-7 human breast cancer cells by observing acoustic streaming around acoustically-excited cancer cells.

1.1. Theory

Here, the theory for predicting the acoustic streaming velocity around the cancer cell is briefly reviewed. In general, the nonlinear acoustic streaming equation is too complicated to be solved directly. Thus, the decomposition of the acoustic streaming equation in terms of pressure (or compressional) and shear wave components was proposed to simplify the equation as well as to improve computational efficiency in solving the decomposed equations [(1)]. In particular, the only compressional wave propagation is assumed outside the thin viscous boundary layer that is formed near to the cell's spherical surface when an acoustic wave incident to the cell interacts with cell's surface vibration. Both the compressional and shear wave propagations are considered within the viscous layer since the spatial change rate (i.e., gradient) of the acoustic streaming velocity is significant only within the viscous boundary

layer. From Doinikov's paper [8], the viscous boundary layer thickness of a compressible cell is given as

$$\delta_v = \sqrt{2\eta\omega/\rho_0}, \tag{1}$$

where δ_v is the viscous boundary layer thickness, η is the dynamic fluid viscosity, ρ_0 is the fluid density, and ω represents the frequency of the excitation wave. Liu and Kim made a further simplification by assuming that the acoustic streaming velocities in the region farther than a certain distance (e.g., $a+10\delta_v$) from the cells can be ignored: i.e., $r < a+10\delta_v$ where a is the radius of the cell and r represents the radius of the effective acoustic streaming region.

The decomposed acoustic streaming equations consist of homogenous and nonhomogeneous parts. Then, the acoustic streaming velocity solution can be represented as a superposition of homogeneous and nonhomogeneous solutions: i.e.,

$$\mathbf{v}_{20} = \mathbf{v}_{20h} + \mathbf{v}_{20p}, \tag{2}$$

where

$$\mathbf{v}_{20h} = \vec{\nabla}\phi_{20h} + \vec{\nabla}\times\boldsymbol{\psi}_{20h} \tag{3}$$

and

$$\mathbf{v}_{20p} = \vec{\nabla}\phi_{20p} + \vec{\nabla}\times\boldsymbol{\psi}_{20p}. \tag{4}$$

In Eqs. (2) – (4), an acoustic variable with the subscript of 20 indicates a second-order, time-independent variable, ϕ is the scalar acoustic streaming velocity potential of the compressional waves, and $\boldsymbol{\psi}$ is the vector acoustic streaming velocity potential of the shear

waves. Since the homogeneous scalar velocity potential ϕ_{20h} is a constant (see Ref. (1)), the homogenous vector velocity potential $\boldsymbol{\psi}_{20h}$ needs to be calculated for $\mathbf{v}_{20h}$ in Eq. (3). This potential is represented in Ref. (1) as

$$\boldsymbol{\Psi}_{20h} = \vec{e}_{\phi} \sum_{n=0}^{\infty} \left(C_{1n} z^{-(n-1)} + C_{2n} z^{-(n+1)} \right) P_n^1 \left(\cos\theta \right), \tag{5}$$

where r and θ are the radial distance and polar angle in the spherical coordinate system, respectively, z is the radial distance normalized by the cell's radius (i.e., $z = r/a$), and is the associated Legendre Polynomials. The coefficients of C_{1n} and C_{2n} can be determined using the vibration velocity boundary conditions on the cell's surface [(1)]. In the nonhomogeneous solution, the scalar velocity potential is represented in Ref. (1) as

$$\phi_{20p} = \sum_{n=0}^{\infty} \left(z^{-(n+1)} \int_{z_{\infty}}^{z} y^{n+2} \mu_n \left(y \right) dy - z^{n} \int_{z_{\infty}}^{z} y^{-(n-1)} \mu_n \left(y \right) dy \right) P_n \left(\cos\theta \right), \tag{6}$$

where

$$\mu_n(z) = \frac{a^2}{2\rho_0} \int_0^{\pi} \vec{\nabla} \cdot \left\langle \rho_1(z) \mathbf{v}_{1\psi}(z) \right\rangle P_n \left(\cos\theta \right) \sin\theta d\theta . \tag{7}$$

In Eq. (7), ρ_1 is the first-order (i.e., linear) acoustic density where the subscript of 1 implies a first-order acoustic variable and $\langle\rangle$ represents the time average over one excitation period. The first-order acoustic variables in Eq. (7) can be calculated from the first-order acoustic wave equations (1). The nonhomogeneous part of the vector velocity potential is calculated in Ref. (1) as

$$\boldsymbol{\Psi}_{20p}=\sum_{n=1}^{\infty}\left(\begin{array}{l}-\dfrac{z^{-(n+1)}}{2(2n+3)}\displaystyle\int_{z_\infty}^{z}y^{n+3}\left(\vec{\chi}_{rn}(y)-(n+3)\vec{\chi}_{\theta n}(y)\right)dy\\+\dfrac{z^{-(n-1)}}{2(2n-1)}\displaystyle\int_{z_\infty}^{z}y^{n+1}\left(\vec{\chi}_{rn}(y)-(n+1)\vec{\chi}_{\theta n}(y)\right)dy\\-\dfrac{z^{n}}{2(2n-1)}\displaystyle\int_{z_\infty}^{z}y^{-(n-2)}\left(\vec{\chi}_{rn}(y)+(n-2)\vec{\chi}_{\theta n}(y)\right)dy\\+\dfrac{z^{n+2}}{2(2n+3)}\displaystyle\int_{z_\infty}^{z}y^{-n}\left(\vec{\chi}_{rn}(y)+n\vec{\chi}_{\theta n}(y)\right)dy\end{array}\right)P_n^1(\cos\theta),\quad(8)$$

where

$$\begin{aligned}\vec{\chi}_{rn}(z)=\frac{\rho_0 a^3}{2\eta}\int_0^{\pi}\vec{e}_r\cdot\Big\langle&\mathbf{v}_1\left(\vec{\nabla}\cdot\mathbf{v}_{1\psi}\right)+\mathbf{v}_{1\psi}\left(\vec{\nabla}\cdot\mathbf{v}_{1\phi}\right)\\&+\left(\mathbf{v}_1\cdot\vec{\nabla}\right)\mathbf{v}_{1\psi}+\left(\mathbf{v}_{1\psi}\cdot\vec{\nabla}\right)\mathbf{v}_{1\phi}\Big\rangle P_n(\cos\theta)\sin\theta d\theta\end{aligned}\quad(9)$$

and

$$\begin{aligned}\vec{\chi}_{\theta n}(z)=-\frac{\rho_0 a^3}{2\eta n(n+1)}\int_0^{\pi}\vec{e}_\theta\cdot\Big\langle&\mathbf{v}_1\left(\vec{\nabla}\cdot\mathbf{v}_{1\psi}\right)+\mathbf{v}_{1\psi}\left(\vec{\nabla}\cdot\mathbf{v}_{1\phi}\right)\\&+\left(\mathbf{v}_1\cdot\vec{\nabla}\right)\mathbf{v}_{1\psi}+\left(\mathbf{v}_{1\psi}\cdot\vec{\nabla}\right)\mathbf{v}_{1\phi}\Big\rangle P_n^1(\cos\theta)\sin\theta d\theta\end{aligned}.\quad(10)$$

In Eq. (8), z_∞ in the integrals is approximated as $z_\infty \cong 1+(10\delta_v/a)$. The equations presented above in this section will be used to predict the resonance frequencies of the MCF-7 cancer cell in the following section.

1.2. Numerical Simulation

The theory presented above is implemented using Matlab (Mathworks). This program is used to simulate the motion of the acoustic streaming around the resonantly-excited MCF-7 cancer cell. The purpose of the simulation is to determine the expected motion of acoustic streaming around a cancer cell and to compare it

with experimentally measured streaming motion. The simulations also allow to estimate the expected resonance frequency range, which can be used as input for the experiments thus reducing the duration of the experiments. Here, the spherical MCF-7 cancer cell is modeled as a homogeneous fluid surrounded by a membrane. In this model, the membrane represents the cell's outer surface. For the numerical simulation results presented below, the diameter of the MCF-7 cancer cells is ranged ranges from 13 μm to 19 μm (mostly around 16 μm), values obtained from direct measurement with a microscope. In the simulation, the speed of sound in the outer fluid medium is given as 1570m/s as in blood since bovine blood was used as part of the liquid medium in the micro-fluidic chip. Commonly-used distilled water could not be used as the liquid medium due to the potential death of the cancer cells during the experiment. The densities of the inner fluid and the outer liquid medium are given as 1068kg/m^3 as in Ref. (11) and 1060kg/m^3 as in blood, respectively. The membrane's surface compression modulus, K_a and surface shear modulus, μ_a are calculated from Eqs. (11) and (12) below [9]. These two updated moduli resulted in 3 - 4 times smaller cell's resonance frequencies than those predicted in the Liu and Kim's paper [1]. The membrane's compression and shear moduli are

$$K_a = Eh / 2(1-v) \tag{11}$$

and

$$\mu_a = Eh / 2(1+v), \tag{12}$$

where E is the Young's modulus, v is the Poisson's ratio, and h is the thickness of the cancer cell's membrane. For the MCF-7 cancer cells, the Young's modulus is set to

1.711 ± 0.864 MPa [10]. The cell's membrane thickness is approximated as one percent of the cell's radius [9]. For example, when the MCF-7 cancer cell's diameter is set to 16 μm, the membrane thickness can be assumed as 80 nm. The Poisson's ratio is typically around 0.5. In order to avoid the singularity problem associated with the Poisson's ratio of 0.5, 0.49 is used in the numerical simulation (see Ref. (1, 11)). Based on the cell modeling parameters above, Eqs. (11) and (12) result in 0.1342 N/m for the surface compression modulus and 0.04593 N/m for the surface shear modulus. The viscosity of the outer fluid medium is given as the blood viscosity of 3.2 cp. The viscosity of the inner cell fluid is given as 9.5 cp since the normal cell's cytoplasm, the fluid within a living cell except the cell nucleus, has the viscosity range of 2 cp to 20 cp [13].

Figure 2 shows the simulation results of with variation of the resonance frequency depending on the cell size. The resonance frequency can be observed at the peak location of the maximum acoustic streaming velocity amplitude in this figure. For the cell with 13.59 μm size diameter, the resonance frequency is observed at 38.98 kHz (ka = 0.0011). For the cells with the diameters of 14.11 μm, 16.54 μm, and 17.52 μm, the predicted resonance frequencies are 37.365 kHz (ka = 0.0011), 30.82 kHz (ka = 0.0010), and 28.665 kHz (ka = 0.0010), respectively. In summary, as one can see in fig. 2, the different size cancer cells can have different resonance frequencies and acoustic streaming velocities, which cannot be ignored. Since the diameter of most MCF-7 cancer cells are measured at around 16μm, the resonance frequencies of MCF-7 cancer cells are expected to be around 29.36 kHz according to the same

simulation process.

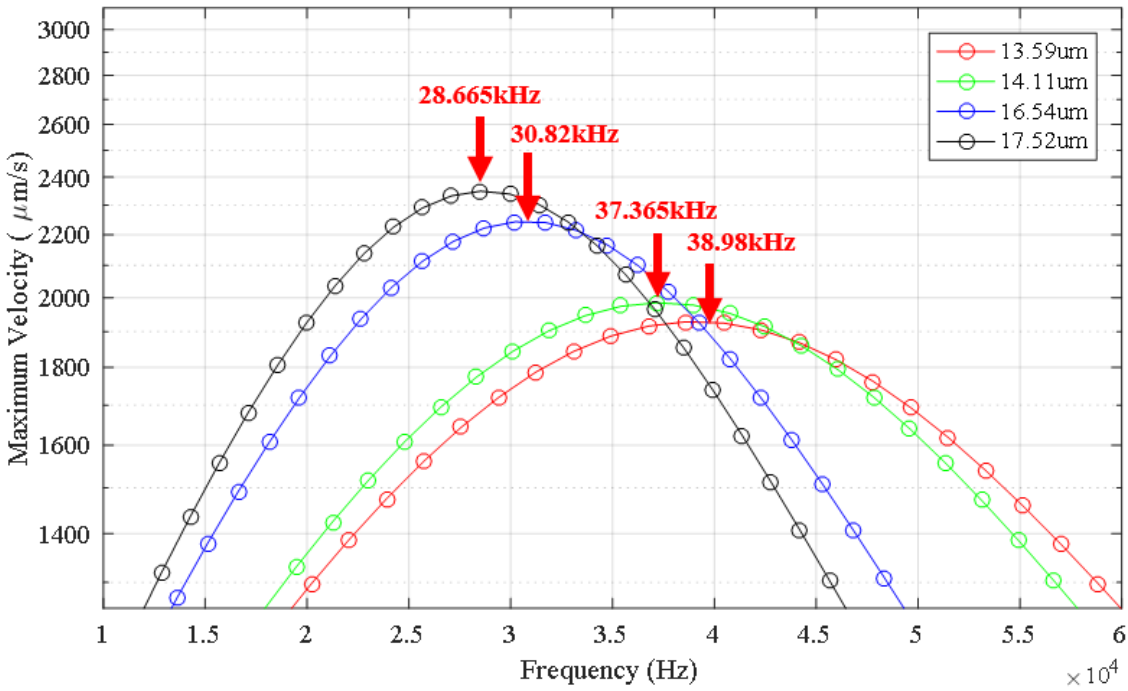

Figure 2. Predicted resonance frequencies of MCF-7 cancer cell with four different diameters of 13.59 μm, 14.11 μm, 16.54 μm and 17.52 μm.

The shift of resonance frequency based on the different size of target cancer cells is also expected in experiment according to this simulation. The decrease of resonance frequency with increase of size of cancer cell can be also intuitively expected since size of an object is inversely related with its fundamental frequency of the object. Figure 3 illustrates the predicted motion of the microparticles flowing along the acoustic streaming around the cancer cell, with the diameter of 16 μm, excited at the resonance frequency of ka = 0.00094 (i.e., 29.36 kHz). As shown in Fig. 3(b) where the arrows represent the acoustic streaming velocities, the streaming velocity

increases as the microparticles flow near the cancer cell and decreases as the particles flow away from the cancer cells: i.e., the arrow size is larger in the area near to the cancer cell than that in the area far from the cell. Thus, similar behavior of streaming velocity change according to the location of particles near the cell is expected in experiment based on this simulation result.

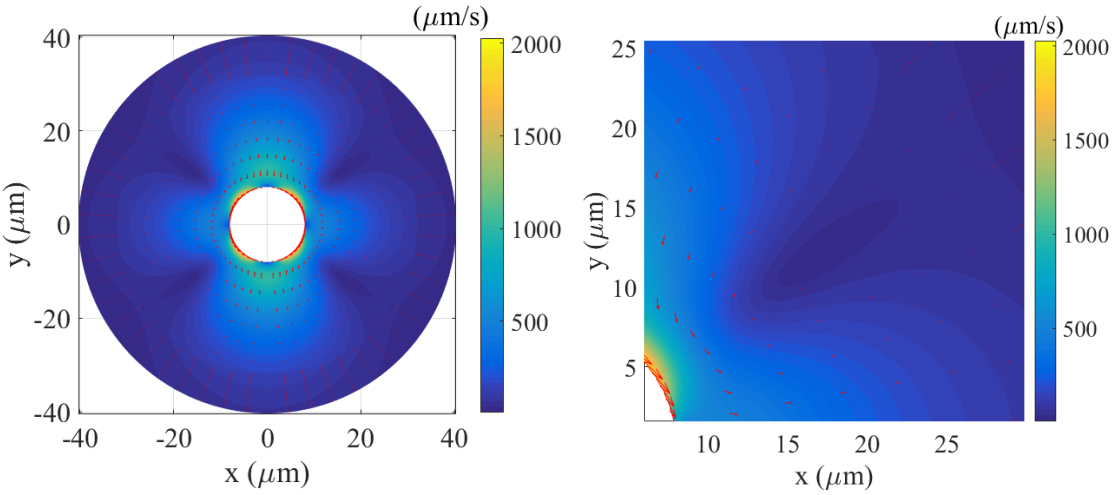

Figure 3. Predicted acoustic streaming velocity around 16 m diameter MCF-7 cancer cell excited at 29.36 kHz: (a) Overall view and (b) Zoomed view near cancer cell surface. The white area at the origin of each plot represents the cancer cell.

2. EXPERIMENT

2.1. Experimental Setup

In order to perform the proposed experiment, it is required to culture the cancer cells and fabricate a microfluidic chip. The purpose of the experiment is to identify resonance frequency of cancer cell. As described in Fig. 1, the cultured cancer cells and microparticles suspended in the cell culture medium are injected into the microfluidic chip though the inlet of the microchip. Then, an acoustic excitation is applied to the microchip through the PZT actuator attached at the bottom of the microchip. There are several advantages related to using a microfluidic device for this experiment. The microchip can be used to prevent the random flows of the beads and cells by guiding the chip's inner liquid flow through its channels and chambers. By preventing random flow inside, the acoustic streaming can be observed more clearly during the experiment. In addition, the microchip can be conveniently used to test multiple targeting beads or cancer cells with the bead and cell flow controlled by the syringe pump. Due to its small size, it also makes possible to consume an extremely small amount of the cells and microparticles.

2.1.1. MCF-7 cancer cell culturing

Several cell culturing processes used for the preparation of this experiment are briefly presented in Appendix A. Each culturing process, even in the experiment itself, requires the use of the cell culture medium. The culture medium for the MCF-7 cancer cells was made by mixing Eagle's Minimum Essential Medium (EMEM), 1% of Glutamine, including Non-Essential Amino Acids (NEAA), and 10% of Fetal

Bovine Serum (FBS).

Since the mechanical properties of cancer cells do not change considerably when their passage number increase, the passage number of cancer cell is not counted in this paper. The passage number of cancer cell indicates the number of how many times the cancer cells were detached from a flask and split into several more flasks in order to give the cells more space to grow in one layer environment. The steps to culture cancer cells, MCF-7, will be explained briefly below. The culturing process for cancer cells are divided into three categories: thawing, subculture, and freezing procedure. The detail steps for culturing cancer cells are shown in Appendix A. Figure 4 briefly illustrates the first thawing step. This step is to defreeze the frozen cancer cells and stabilize to make the cancer cells grow again.

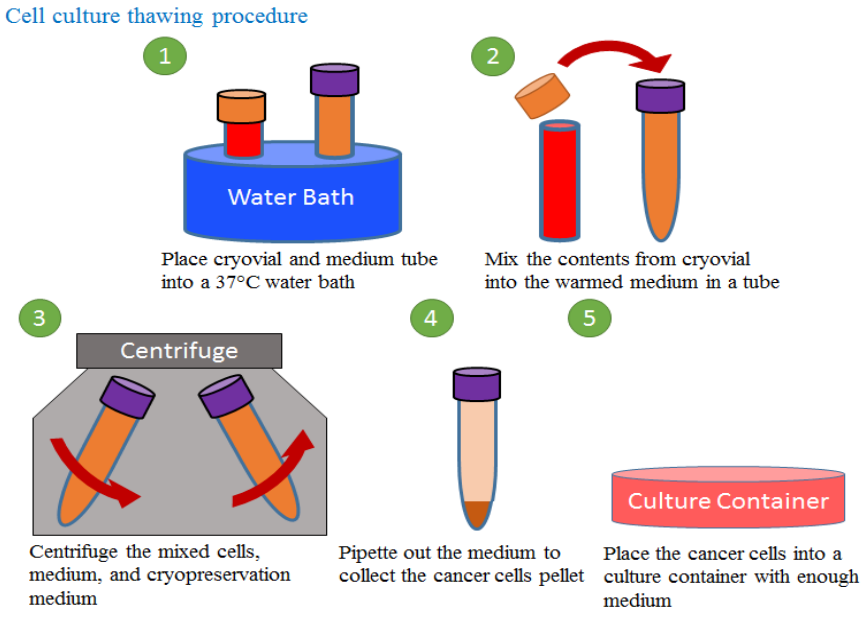

Figure 4. Cell culture thawing procedure

Figure 5 clearly explains the sub-culturing procedure. The more detail steps are attached in appendix A. This step is to culture cancer cells to obtain more amount of the cancer cells. The sub-culturing should be done before the culture container is filled with the cancer cells in one layer.

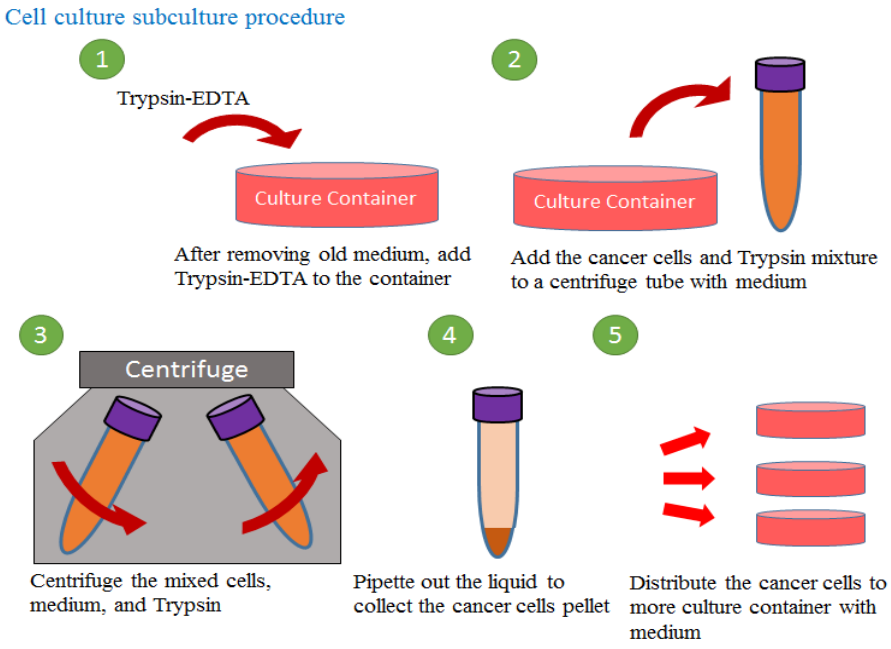

Figure 5. Cell culture subculturing procedure

The last step of culturing cancer cell is freezing. This step is to simply make the cancer cells frozen to store it safely for later usage.

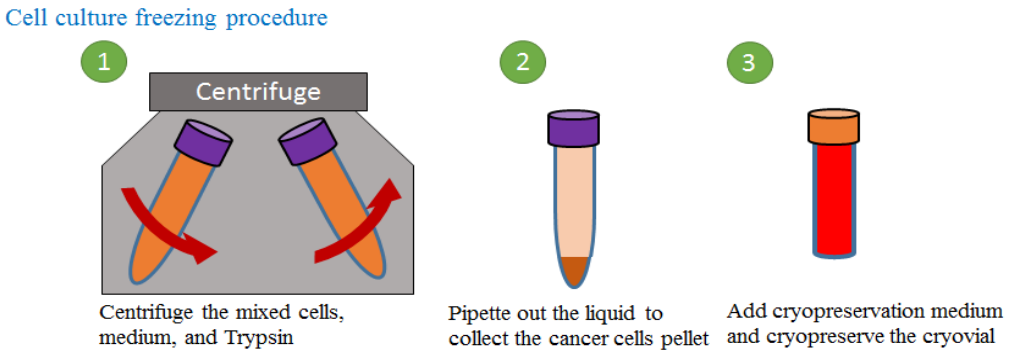

Figure 6. Cell culture freezing procedure

2.1.2 Design and fabrication of microfluidic, acoustophoretic device

For the microfluidic device fabrication, Polydimethylsiloxane (PDMS) material is used since this material is cheap and easy to handle. It is transparent and bio-compatible and also can be bonded tightly with silicon, glass or other PDMS layer with a simple plasma treatment. In this paper, a fabrication method based on a silicon PDMS mold was adopted to fabricate the PDMS-silicon microfluidic device. Although a glass cover and an etched silicon channel also could be bonded and used as an acoustophoretic device for this experiment, due to their efficient acoustic wave transmission, these fabrications were not adopted in this paper because they require comparably more times than PDMS silicon fabrication process. The PDMS microfluidic device fabrication methods have three main steps: (1) Master mold fabrication, (2) PDMS channel fabrication, and (3) Oxygen plasma bonding process. More detail fabrication process is given in Appendix B. Figure 7(a) shows the fabricated PDMS-silicon microchip. As shown in Fig. 7(a), the microchip consists of one inlet and one outlet (with tubes attached), one straight channel, two circular

chambers to reduce air bubbles, and one circular observation chamber. Figure 7(b) shows the microscopic image of the circular observation chamber inside the PDMS-silicon chip with the cancer cells and microparticles injected. The relatively big circles are the MCF-7 cancer cells and the small dots represent the 2 μm diameter microparticles.

The overall actual experimental setup is shown in Fig. 8. The overall experimental procedures are briefly presented in Fig. 1 above. The PZT actuator was used to excite the microchip at a single frequency per each excitation step in the frequency range from 20 kHz to 130 kHz with 100 Hz step size with power around 15 W. In order to avoid the resonance frequency shift induced by the elevated temperature of the PZT actuator, the excitation was stopped at every 20 seconds to lower (cooldown) the temperature of the device.

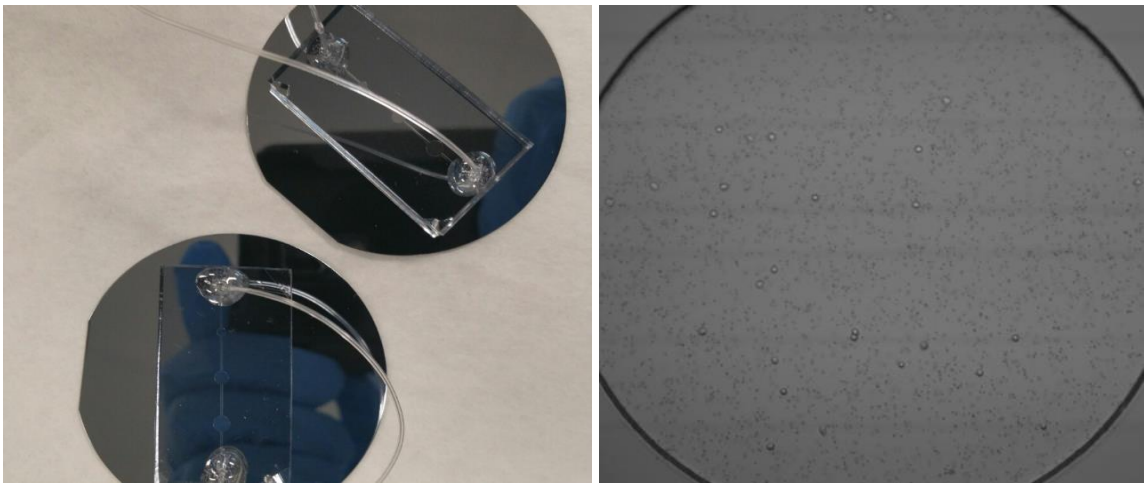

(a) (b)

Figure 7. (a) Silicon mold based PDMS-silicon chip and (b) Microscopic view of circular observation chamber in PDMS-silicon chip with MCF-7 cancer cells and microparticles injected.

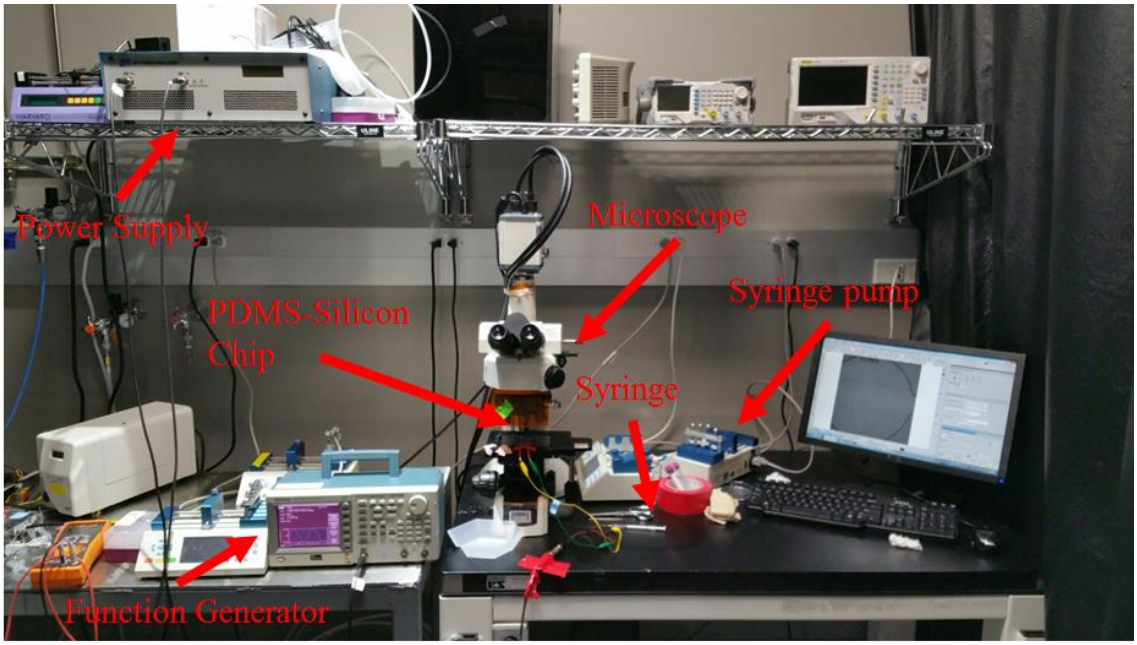

Figure 8. Experimental setup for validation of resonantly excited cancer cells

2.2. Experimental Results and Discussion

At 28.7 kHz, 31.1 kHz, 36.9 kHz, and 42.0 kHz frequency excitations, the rotational motions of 2 μm microparticles around the MCF-7 cancer cells with the average diameters of 17.52 μm, 16.54 μm, 14.11 μm, and 13.59 μm were observed, respectively, as shown in Table 1. Cancer cells with higher diameter have higher maximum velocity, leading to the microparticles' rotation generation in wider range of frequencies while the rotation phenomenon around low diameter cancer cells is generated only at the peak of maximum velocity. In the case of wide range of frequencies with higher diameter cancer cells, mid-point of the frequency range (peak point) is chosen as the resonance frequency. Figure 9 illustrates that the resonance frequency of the cell decreases as the size of the cell increases. It is also shown that

the predicted frequency matches well with the measured frequency within the difference of approximately 0.5 kHz except the cell with the diameter of 13.59 μm. Overall, the experimental proved that Liu and Kim's theoretical method results don't have statistically significant difference from the experiment results based on T-test where alpha of 0.05 leads to t-value of 1.8435. The t-value is not large enough to be significant. Fig. 10 shows the microparticle's motion at 1 frame/second around the cell with the diameter of 17.52 μm and the resonance frequency of 28.7 kHz and Fig. 11 shows the trajectory of this microparticle in a single plot. According to fig 10 and 11, the velocity of the acoustic streaming is higher near the cancer cell and lower in further region.

Table 1 – Predicted and measured resonance frequencies of MCF-7 cancer cells with four different diameters.

Average Size of resonantly excited MCF-7 cells (μm)	17.52	16.54	14.11	13.59
Predicted by Simulation	28.665kHz	30.82kHz	37.365kHz	38.98kHz
Experimentally Measured	28.7kHz	31.1kHz	36.9kHz	42.0kHz

As shown in these two figures, the microparticle moves faster near the cancer cell, while its motion is getting slower as the microparticle moves farther away, as expected from the numerical simulation. As expected from figure 2 graph, the maximum velocity of acoustic streaming varies according to the size of the cancer cells also.

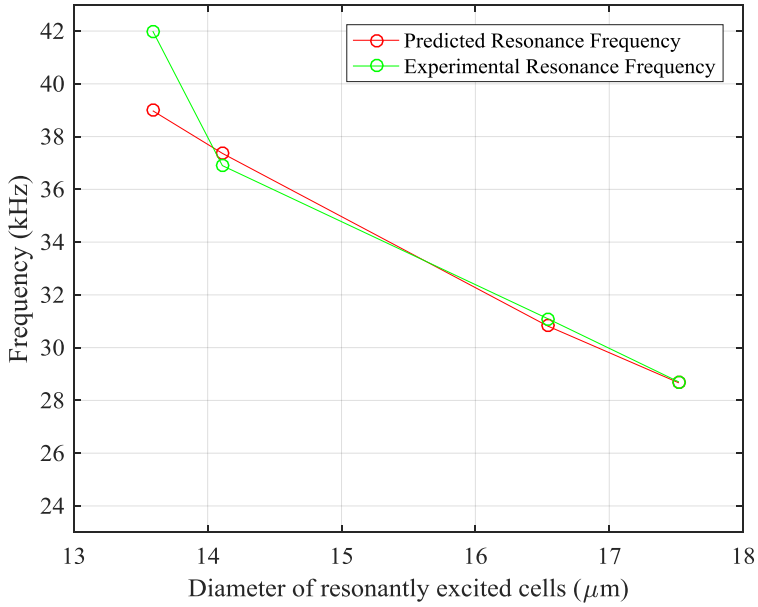

Figure 9. Predicted and measured resonance frequencies of MCF-7 cancer cells with four different diameters of 13.59 μm, 14.11 μm, 16.54 μm, and 17.52 μm. This plot was generated from the information in Table 1.

Through the observation of the microparticles' rotational motion around the MCF-7 in both the simulation and experiment at similar resonance frequencies, it is shown that the theoretical approach proposed by Liu and Kim [(1)] don't have statistically significant difference from the experiment results so it can be used to predict the acoustic streaming velocities and the resonance frequencies of the cancer cells. It is also proved that the proposed experimental method for finding the resonance frequencies of the cancer cells is viable.

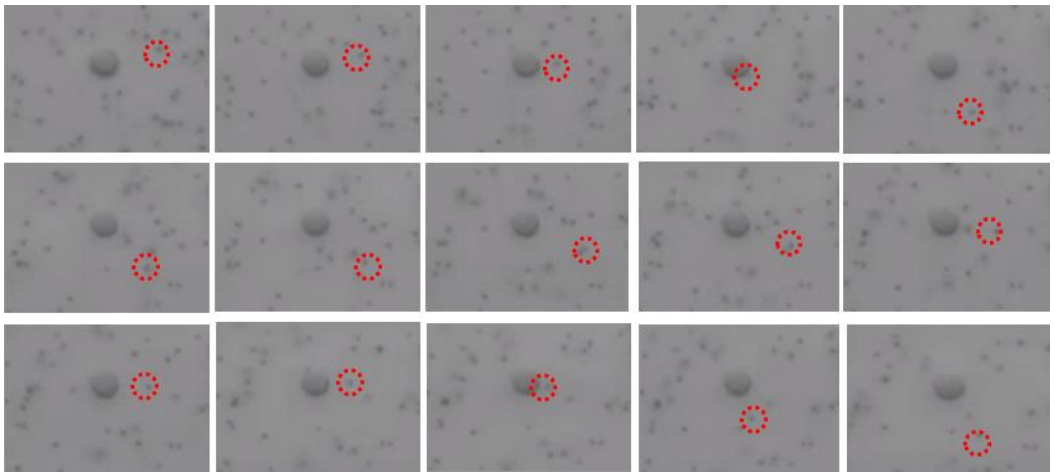

Figure 10. Motion of microparticles around resonantly-excited MCF-7 cancer cell with diameter of 17.52 μm at 1 frame/second. The excitation frequency is 28.70 kHz.

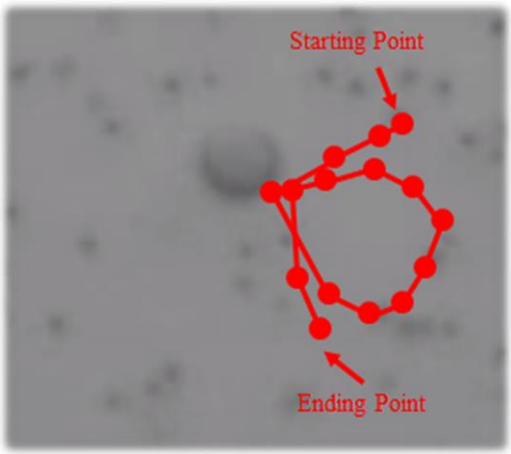

Figure 11. Trajectory of the microparticles around the resonantly excited MCF-7 cancer cell. The dots represented the locations, of the microparticles, sampled at 1 frame/seconds for 15 seconds.

3. MIGRATION OF PARTICLES TO THE CENTER SIMULATION

In a thesis paper, "Acoustophoresis of microparticles and cells in microfluidic devices" by Liu [14], a new microfluidic device design is introduced. This device can separate cells/microparticles according to their different compressibility, density, and size by controlling the speed of the fluid flow and applied acoustic wave inside of the channel. In this section, additional works that has been done to improve the accuracy of the separation device. The process used to fabricate the separation channel will be briefly introduced.

The control factors that a separation device uses to separate cells/microparticles are acoustic force and fluid speed from inlet to outlet. In the Liu's simulation, the flow speed velocity of microparticles is assumed to be constant. However, in a microfluidic channel, the flow speed of microparticles varies depending on their location inside the channel due laminar flow effect. Thus migration of microparticles to the cross-sectional center of the microfluidic device has to be done to avoid cell/microparticles' irregular flow velocities.

3.1. Simulation Results

The Liu's separation device [14] assumes that the flow of cells/microparticles starts at the same location. Therefore, both horizontal and vertical nodal line acoustic forces have to be properly applied to the microparticles in order to make the cells/microparticles to move to the same location in cross-sectional location of the channel (center of the channel). In figure 12, two acoustic forces that can be used to move cells/microparticles at the center of the channel (in cross-sectional view of the

microfluidic channel) are used. The left acoustic force is used to move cells/microparticles to the middle of the channel, and the right acoustic force works as levitational acoustic force.

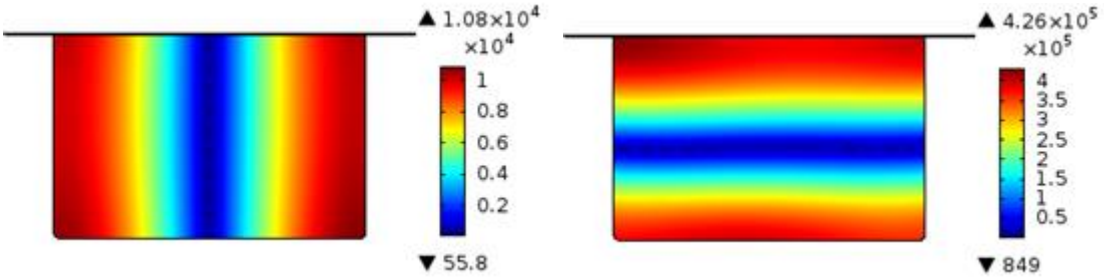

Figure 12. Nodal lines created for 0.3186 MHz and 0.4898 MHz in 2.3x1.7mm channel size device.

Here, a channel with width of 2.3 mm and height of 1.7 mm is simulated. The dimension of the channel is much bigger than what introduced in the Liu's paper. This increase of dimension is necessary in order to reduce overall noise, which can affect the actual experiment. The expected resonance frequencies of the channel can be calculated by dividing speed of sound in the channel fluid by two times the length of the dimension.

3.2 Discussion

In order to verify that simulation results of two vertical and horizontal nodal lines can be used to move targeting micro-objects to cross-sectional center of the microfluidic channel, experimental process and results have to be compared with the simulation results. However, in this chapter, only the simulation and preparation of experiment setup are discussed. Since 1.7mm depth of microfluidic channel is hard to fabricate by silicon

etching technique due to RIE etching machine's limitation, micro-milling process can be applied to materials such as aluminum for the fabrication of the device.

After the fabrication of device, bonding between transparent cover and the micro-milled aluminum device has be formed. However, common oxygen plasma process which is used to create a bond between PDMS and silicon can't create bonding that is strong enough between aluminum and transparent cover such as glass. According to Sunkara and Park's work, APTES solution can be applied in order to create irreversible bonding between PDMS and aluminum after the oxygen plasma process between the PDMS and aluminum [(15)]. Thus, a thin layer of PDMS is desired to be fabricated first and attached to a glass cover with oxygen plasma process. Then, the thin layer of PDMS side of the glass-PDMS can be later bonded with aluminum channel side through the APTES and oxygen plasma processes which is introduced in Ref 15.

4. CONCLUSION

In this thesis, an experimental method is proposed to identify the resonance frequencies of a cell/particle by observing the rotational motion of microparticles around the cell/particle. Based on the numerically-predicted and experimental results, the resonance frequency of the MCF-7 cancer cells can be identified in the range 39 kHz to 29 kHz for cell diameters in the range 14 μm to 18 μm, respectively. It is also shown that the resonance frequency is inversely proportional to the cell diameter. In the future, the measured resonance frequencies can be used to estimate various mechanical properties of cancer cells. This study proves the feasibility of the proposed experimental method for finding the resonance frequencies of the cancer cells. Statistical analysis demonstrates no significance difference between the resonance frequencies obtained through the experimental observations of the microparticles' rotational motion around the MCF-7 and the simulations based on the theoretical model. Thus, the theoretical approach proposed by Liu and Kim [1] can be used to predict the acoustic streaming velocities and the resonance frequencies of the cancer cells. In addition, the work reported in this thesis show that two nodal lines can be generated at the cross-section of a rectangular micro-fluidic channel, and that it is possible to move the microparticles/cells to the cross-sectional center of a microfluidic device with two acoustic waves of two different frequencies. So far, this problem has been studied using simulations. In the future, fabrication of a device and experiment verification are required to corroborate the simulation results.

REFERENCES

1. Liu, Z and Kim, Y.-J. Acoustic streaming around a spherical microparticle/cell under ultrasonic wave excitation. Proc INTER-NOISE 2015; San Francisco, California 2015. 17, p. 98-125.

2. Ackerman, E. Mechanical resonances of amphiuma erythrocytes. J. Acoust. Soc. Am.; 1954. 26, p. 257-258.

3. Marston, L. and Apfel, R.E. Acoustically forced shape oscillation of hydrocarbon drops levitated in water. J. Colloid Interface Sci; 1979. 68, p. 280-286.

4. Chung, S and Cho, Sung. On-chip manipulation of objects using mobile oscillating bubbles. Journal of Micromechanics and Microengineering; Pittsburgh 2009. 18, p. 1-12.

5. Ahmed, D and Ozcelik, A. Rotational manipulation of single cells and organisms using acoustic waves. Nature Communication; Pennsylvania 2016. 7, p. 1-11.

6. Wiklund, M and Green, R. Acoustofluidics 14: Applications of acoustic streaming in microfluidic devices. Lab Chip; 2012. 12, p. 2438-2451.

7. Dai, L and Jiao, N. A Micromanipulator and Transporter Based on Vibrating Bubbles in an Open Chip Environment; Micromachines 2017; 8, p. 130.

8. Doinikov, A.A. Acoustic radiation pressure on a compressible sphere in a viscous fluid. J. Fluid Mech; 1994. 267, p. 1-22.

9. P.V. Zinin, J.S.A III and V.M Levin. Mechanical resonance of bacteria cells. Phys. Rev. E; 2005. 72, p. 72.

10. Yallapu, M., Katti, K., Katti, D., and Mishra, S. The roles of cellular nanomechanics in cancer. Med Res Rev; 2015 Jan. 35, p. 198-223.

11. Dokukin, M., Guz, N., and Sokolov, I. Quantitative study of the elastic modulus of loosely attached cells in AFM indentation experiment. Biophys J; 2013 May 21. 104, p. 2123-2131.

12. Hartono, D., Liu, Y., Tan, P.L., Yung, L., and Lim, K.M. On chip measurements of cell compressibility via acoustic radiation. Lab Chip; 2011. 23, p. 4072-4080.

13. Arrio-Dupont, M., Cribier, S., Foucault, G., Devaux, P., and d'Albis. A. Diffusion of fluorescently labeled macromolecules in cultured muscle cells. Biophysical Journal; 1996 May. 70, p. 2327-2332.

14.Liu. Z. Acoustophoresis of Microparticles and Cells in Microfluidic Devices. A Dissertation; Texas A&M University Aug 2016. 199, p. 98-133.

15.Sunkara. V, Park D.K., and Cho Y.K. Versatile method for bonding hard and soft matrials. RSC Advances; 2012. 2, p. 9066-9070.

APPENDIX A

MCF-7 HUMAN CANCER CELL CULTURING PROCESS

A. Cell Culture Thawing Procedure: Thawing is a part of culturing process which defreeze frozen cancer cells and removes cryopreservation media, including toxic dimethyl sulphoxide (DMSO) media and eventually plate the cells in flask with culture medium. The more detail steps are written following:

1. EMEM medium mixture which is liquid designed to support the growth of cells are placed into a 37°C water bath.

2. The cryovial, which contains the frozen cancer cells with cryopreservation media, is placed into the 37°C water bath to defreeze the frozen cells.

3. The cryovial contents are transferred to the pre-warmed medium in a 15ml tube.

4. The tube is centrifuged at 1000rpm for 5 minutes to collect the cancer cells pellet.

5. After pipetting out the separated medium and cryopreservation media, 1ml of EMEM medium mixture is pipetted into the tube and mixed with the cancer cells.

6. The cancer cells and medium mixture are placed into a flask or a culture vessel with more medium (amount depending on the size of the culture vessel or flask).

7. Wait for the adherent cancer cells to be stabilized.

B. Cell Culture Subculture Procedure: After the cancer cells are grown in a few days, the culture container can be too small for the grown and crowded cancer cells. This crowding can be lethal to the cancer cells, possibly leading to the cancer cell's death due to the insufficient nutrient for the increased number of cells. Thus, the crowded cancer cells are recommended to split into two or more new containers with new fresh medium.

If the cancer cells are adherent cells, they first have to be detached from their flask or culture vessel. Trypsin is proteolytic enzyme which helps to break protein to lead to the cancer cell detachment.

1. EMEM medium mixture and trypsin-EDTA are placed in 37°C (room temperature) water bath for pre-warmup. Room temperature is required to prevent death of cancer cells when the liquid is mixed with the cancer cells.

2. The old medium from the culture flask or a culture vessel is pipetted out, leaving only cancer cells that are attached on the container.

3. Pipette phosphate-buffered saline (PBS) (amount depending on the size of the container) into the flask and pipette out the PBS to the bleach bottle. Repeat this step one more time. This step is required to clean out the old medium, dead cancer cells and residues of cancer cells. PBS is isotonic and non-toxic to most cells. It is appropriate for cleaning for cancer cells.

4. Add trypsin (amount depending on the size of the container) into the flask or container and keep the flask in the incubator about 5mins. This step is to detach the adherent cancer cells from the bottom of a flask. The trypsin breaks the protein which helps the detachment.

5. Add medium mixture into the flask and move the mixture of trypsin+ medium + cancer cells into centrifuge tube and centrifuge the tube at 1000 rpm for 5 mins to collect the cancer cells pellet only later.

6. Pipet out the medium and trypsin.

7. Add 1ml of new fresh medium into the flask and gently shake it with an aspirator to mix the cancer cells with the fresh medium.

8. Distribute the mixture to more culture vessels as user wants: e.g. if distribution into 5 flasks. Each flask will contain 0.2 ml of the mixture of the cancer cells and 1ml of fresh medium. More medium has to be added more to each of the container to give enough nutrient to the cells. Or it can be used directly for the experiment without additional medium.

C. Cell Culture Freezing Procedure:

1. The old medium from the culture flask or a culture vessel is pipetted out, leaving only cancer cells that are attached on the container.

2. Pipette phosphate-buffered saline (PBS) (amount depending on the size of the container) into the flask and pipette out the PBS to the bleach bottle. Repeat this step one more time. This step is required to clean out the old medium, dead cancer cells and residues of cancer cells. PBS is isotonic and non-toxic to most cells. It is appropriate for cleaning for cancer cells.

3. Add trypsin (amount depending on the size of the container) into the flask or container and keep the flask in the incubator for 5minutes. This step is to detach the adherent cancer cells from the bottom of a flask. The trypsin breaks the protein which helps the detachment.

4. Add medium into the flask and move the mixture of trypsin+ medium + cancer cells into centrifuge tube and centrifuge the tube at 1000 rpm for 5 mins to collect the

cancer cells pellet only later. (The medium is added to the mixture to neutralize the trypsin).

5. Gain the cancer cell pellet only by pipetting out the trypsin and medium into a cryovial.

6. Add cryopreservation media such as DMSO which prevent the ice crystal damaging the cells when it is cooled down.

7. A vial is cooled down in certain rate (usually -1°C per minute) to freeze it.

APPENDIX B

FABRICATION OF MICROFLUIDIC DEVICE

A. 3D printed mold based PDMS micro-fluidic Chip: 3D printing mold is much faster to fabricate than the Silicon mold; however, its resolution is much lower than the silicon mold.

1. Master mold fabrication:

a. The software design file for the 3D print has to be made first. The thickness of the mold has to be at least more than 7mm in order to prevent any possible cracks on the mold when the PDMS is solidified and expanded on the mold. The eight hexahedron shapes around the channel exist also to let the PDMS to expand through the space between to prevent possible cracks.

b. After the 3D printing, the mold has to be exposed to UV light in order to harden the mold.

2. PDMS channel fabrication:

a. The master mold and an experiment boat with a few drops of Trichlorosilane are placed in degassing chamber to cover the mold surface with Trichlorosilane so the hardened PDMS can be taken apart from the mold easily later.

b. Sylgard 184 polymer resin and curing agent must be mixed in 10:1 ratio. If the ratio of curing agent to base is increased, the layer gets harder, more cross-linked elastomer results.

c. The mixture is placed in a degassing chamber to remove bubbles inside.

d. The side of the mold is taped so the PDMS will expand easily through the tapes.

e. The degassed mixture is then poured on the mold and the mold with mixture is placed in the degassing chamber to completely remove bubbles inside.

f. The mold with degassed PDMS is then placed in an oven to hardening.

g. After more than 12 hours, the PDMS can be taken apart.

h. With golden needles, the inlets and outlets of the PDMS can be punched.

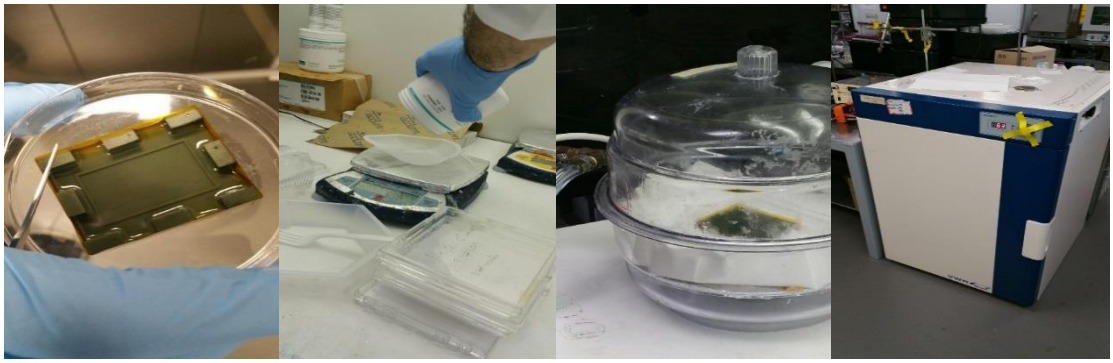

Figure 13. Fabricated mold → PDMS forming → Degassing → Baking

3. Oxygen Plasma bonding process:

a. A glass or a silicon wafer and the punched PDMS channel are placed in bonding side up in Oxygen Plasma chamber for 2 mins in 1 oxygen pressure. The plasma treatment will modify the surface chemicals and allows to stick the PDMS with the channels against other substrates (PDMS, silicon or glass).

b. The glass or silicon and PDMS are bonded together tightly and tubes are injected into the inlets and outlets of the microfluidic chip.

c. The Silicon-PDMS or Glass-PDMS chip is then placed in an oven for 12 hours for a final complete hardening.

Figure 14. Fabricated Glass-PDMS microfluidic chip and surface of the channel through a microscope

As one can notice from above steps and figures, the 3D-printed mold based microfluidic chip can be fabricated faster compare to other chip fabrication methods; however, due to the limit of 3D printing technique, the resolution of the chip is lower than the other method based microfluidic chips. From figure 14, it is noticeable that there the surface of the chip is not smooth and some rectangular traces are made on the surface of the channel due to the 3D printer's limit.

B. Silicon mold based PDMS micro-fluidic Chip: Silicon mold based PDMS channel has much higher resolution than the 3D printing mold. However, there is height limitation for the channel depth due to the viscosity of SU-8. The only difference of the silicon mold based PDMS micro-fluidic chip fabrication method from the 3D printed based micro-fluidic chip is only the first mast mold fabrication step.

1. Master mold fabrication:

a. First, the silicon has to be pre-processed to be cleaned by applying acetone, isopropanol and DI water.

b. Negative photoresist is poured on the center of the silicon wafer. In this experiment SU-8 2075 negative photoresist was used. Although both postive and negative photoresist can be used for the fabrication of a silicon mold and although the positive photoresist generally results higher resolution, the positie photoresist is undesirable to be used in the silicon mold because of its low viscosity. To give some height of to the mold, certain high viscosity has to be used. In our case SU-8 2075 has 22000 cSt viscosity. The design of our channel has one inlet, one outlet and three different size circular chambers. The big first two circular chambers work as a filter for air bubbles, and the last smallest circular chamber is to observe the rotation phenomemnon.

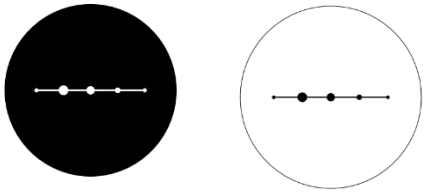

Figure 15. Negative photoresist mask, Positive photoresist mask

The silicon wafer is then spin-coated to remove air bubbles inside of the photoresist and space between the photoresist and the silicon wafer. The spin-coating also makes the photoresist spread uniformly on the surface of the silicon wafer. The thickness of the photoresist can be controlled by controlling the spin speed. For our case, 3000 rpm was used to result 75um thickness. Since the general diameter of MCF-7 cancer cells are about 10um. The thickness is enough for the cancer cells to pass through. After the PDMS

hardening the channel height would be reduced to around 50~60um because of the PDMS expansion.

c. Soft bake step is then applied to make the sticky photoresist to be hardened and spread more uniformly. This step is also important because it prevents the wafer sticking to the mask during the UV exposure process. In our case, 3mins of 65°C and 8minutes of 95°C was applied.

d. After the soft bake, the wafer is exposed to UV light. The negative photoresist mask from figure 14 leads only the channel to be exposed to the light and hardened. In our case, 65 seconds for 3.7mW/cm2 power was used so it would give about 250.5 mJ/cm2.

e. After the UV exposure, post exposure bake step is applied to re-hardens the exposed region more. In our case, we used 3 minutes of 65°C and 16 minutes of 95°C.

f. Developer process is applied then to remove all the photoresist where it was not exposed to the UV-light.

g. Finally, 30 minutes of 135°C of hard baking was applied to the wafer for hardening.

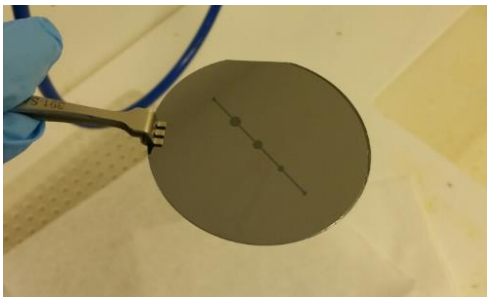

Figure 16. Fabricated silicon mold with Negative photoresist

The next PDMS channel fabrication and oxygen plasma bonding methods for the silicon mold based microfluidic chip are same as what was explained above from the 3D printed mold based microfluidic chip. PDMS can be poured on both of the molds to fabricate the channels.

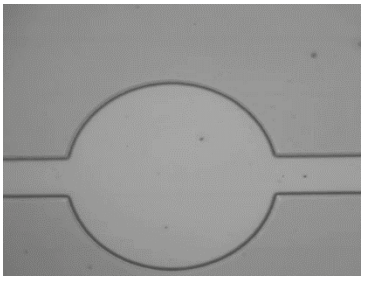

Figure 17. Silicon mold based microfluidic device

As one can notice from figure 14 and figure 17, the channel resolution of the silicon mold based micro-fluidic chip is much higher than the channel resolution from the 3D printed based micro-fluidic chip. In our experiment, the silicon mold based micro-fluidic chip was used because the small cracks or rectangular traces of the 3D printed mold based PDMS channel could result random acoustic streaming around the cracks which can possibly interrupt the observation of the beads rotation and attraction.